A window into the complexity of the dynamic rupture of the 2011 Mw 9 Tohoku-Oki earthquake

Lingsen Meng,[1] Asaf Inbal,[1,2] and Jean-Paul Ampuero[1]

Received 16 May 2011; revised 20 July 2011; accepted 20 July 2011; published 24 August 2011.

[1] The 2011 Mw 9 Tohoku-Oki earthquake, recorded by over 1000 near-field stations and multiple large-aperture arrays, is by far the best recorded earthquake in the history of seismology and provides unique opportunities to address fundamental issues in earthquake source dynamics. Here we conduct a high resolution array analysis based on recordings from the USarray and the European network. The mutually consistent results from both arrays reveal rupture complexity with unprecedented resolution, involving phases of diverse rupture speed and intermittent high frequency bursts within slow speed phases, which suggests spatially heterogeneous material properties. The earthquake initially propagates down-dip, with a slow initiation phase followed by sustained propagation at speeds of 3 km/s. The rupture then slows down to 1.5 km/s for 60 seconds. A rich sequence of bursts is generated along the down-dip rim of this slow and roughly circular rupture front. Before the end of the slow phase an extremely fast rupture front detaches at about 5 km/s towards the North. Finally a rupture front propagates towards the south running at about 2.5 km/s for over 100 km. Key features of the rupture process are confirmed by the strong motion data recorded by K-net and KIK-net. The energetic high frequency radiation episodes within a slow rupture phase suggests a patchy image of the brittle-ductile transition zone, composed of discrete brittle asperities within a ductile matrix. The high frequency is generated mainly at the down-dip edge of the principal slip regions constrained by geodesy, suggesting a variation along dip of the mechanical properties of the mega thrust fault or their spatial heterogeneity that affects rise time.
Citation: Meng, L., A. Inbal, and J.-P. Ampuero (2011), A window into the complexity of the dynamic rupture of the 2011 Mw 9 Tohoku-Oki earthquake, *Geophys. Res. Lett.*, *38*, L00G07, doi:10.1029/2011GL048118.

1. Introduction

[2] The Mw 9 earthquake that occurred off-shore Tohoku, Japan, on March 11 2011 is by far the best recorded earthquake in the history of seismology and will undoubtedly spawn a broad range of studies that will deeply transform earthquake science. In particular, this event provides a unique opportunity to address, through high resolution and robust observations, fundamental questions about the physics of dynamic earthquake rupture, including the initiation of rupture, the complexity of its propagation and its arrest. Here we focus on key direct observations of the spatio-temporal evolution of the rupture process of the Tohoku earthquake. We analyze seismic data available soon after the event using source imaging methods that are weakly dependent on model assumptions. We back-projected teleseismic waveforms applying high-resolution array processing techniques to obtain a high-frequency image of the rupture process of this mega-earthquake. We then identified prominent features of the local strong-motion recordings that we associate to the main phases of the rupture process. Our results reveal, with unprecedented detail, rich patterns of high frequency radiation from the deep portions of the seismogenic zone. Our observations open a direct window into the complexity of dynamic rupture, including phases of slow and extremely fast rupture, and its relation to the heterogeneous nature of the subduction interface.

[3] Back-projection of high-frequency (HF) seismic waves recorded by dense arrays [*Fletcher et al.*, 2006; *Ishii et al.*, 2005] deliver unique insights on earthquake rupture processes that are complementary to traditional finite source inversions. Array back-projection aims at tracking the areas of the source that generate the strongest high frequency radiation, based solely on the phase and the coherency of seismic array signals. This provides robust constraints on the spatio-temporal evolution of the earthquake rupture, without relying on assumed Green's functions nor on restrictive parameterizations of the rupture kinematics. We back-projected P wave seismic waveforms recorded by two large arrays at teleseismic distances, the USarray and the European network, that illuminate the fault from two orthogonal directions (Figure 1). We causally filtered the waveforms from 0.5 to 1 Hz, the highest band in which the initial arrivals are coherent to be aligned robustly. We then applied three different array processing techniques: cubic-root stacking [*Rost and Thomas*, 2002], a classical beamforming technique; Multiple Signal Classification (MUSIC) [*Goldstein and Archuleta*, 1991; *Schmidt*, 1986], a high-resolution technique designed to resolve closely spaced simultaneous sources; and correlation stacking [*Borcea et al.*, 2005; *Fletcher et al.*, 2006], a technique known to improve robustness in the presence of scattering. The detailed descriptions of the techniques are included in the auxiliary material.[1] Our results based on these three techniques are mutually consistent (Figures 1, 2, S1 and S2 of the auxiliary material). Nevertheless, we found that MUSIC consistently yields a sharper image of secondary features of the rupture process. We back-projected the estimated directions of arrival onto the source region using

[1]Seismological Laboratory, California Institute of Technology, Pasadena, California, USA.
[2]Department of Geological and Environmental Sciences, Ben-Gurion University of the Negev, Beer-Sheva, Israel.

0094-8276/11/2011GL048118

[1]Auxiliary materials are available in the HTML. doi:10.1029/2011GL048118.

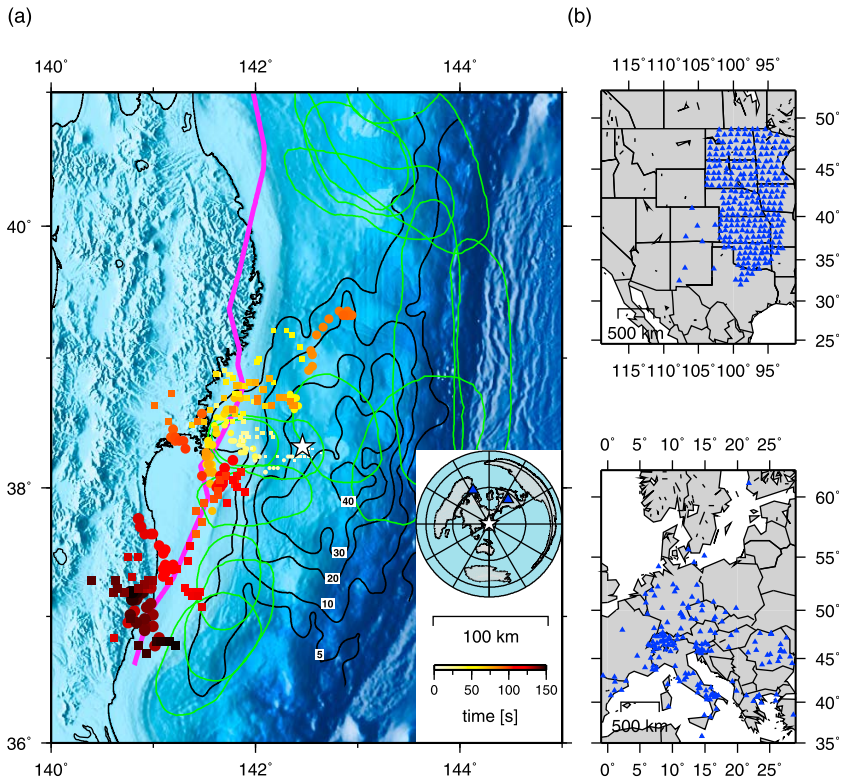

Figure 1. Tohoku-Oki earthquake imaged by the USarray and European network. (a) Location of the strongest high frequency radiators of the Tohoku-Oki earthquake, seen by the USarray (squares) and by the European network (circles). The color denotes the timing with respect to the origin time. The size of the symbols denotes the relative amplitude of the radiators. The black contours map the average slip distribution constrained by geodetic and tsunami data [*Simons et al.*, 2011]. The green ellipses represent the approximate rupture zone of the historical earthquakes. The pink line near the coast indicates the down-dip limit of the megathrust seismicity [*Igarashi et al.*, 2001]. The inset map shows the location of the two arrays with respect to Japan. (b) Location of the 291 USarray and 181 European stations selected for our back-projection analysis.

differential travel times relative to the hypocentral travel time, based on the IASP91 Earth model. Due to the lack of sensitivity of differential travel times to source depth, we project the array images at an arbitrary reference depth of 15 km. We focus on features of the rupture process that are consistently imaged by both arrays. Remaining differences can be attributed to directivity effects, to interference patterns between direct and depth phases and to geometrical properties of the isochrones [*Bernard and Madariaga*, 1984; *Spudich and Frazer*, 1984]. Owing to its larger aperture, the European array provides a sharper image of the rupture process. Our synthetic tests based on empirical Green's functions (Figures S4–S7 of the auxiliary material) show that our back-projection imaging can capture the key features of the rupture process of the Tohoku-Oki earthquake highlighted next.

2. High Resolution Array Analysis Using USarray and European Network

[4] Figure 1a shows the location of the regions of strongest HF radiation within 10 seconds long sliding windows. Secondary sources are often visible in our back-projection images, for instance in Figure 3 between 60 and 90 seconds. However, our focus here is on first order features that we can reliably identify by tracking the most coherent phase within each time window. The HF radiation area extends bilaterally over 300 km along strike, roughly one third to the NNW direction and two thirds to the SSE. It bridges over the rupture area of several historical earthquakes off-shore Miyagi and Fukushima that were previously thought to define the segmentation of this subduction interface. The HF rupture is mostly located landwards of the hypocenter, near the down-dip end of the seismogenic zone of the megathrust interface determined from the spatial distribution of megathrust seismicity in the last decades [*Igarashi et al.*, 2001]. Figure 1a also shows the spatial distribution of coseismic slip averaged over a large collection of possible models constrained by geodetic (GPS) and tsunami (DART buoy) data in a Bayesian framework [*Simons et al.*, 2011]. The locations of HF sources correlate with the down-dip edge of the main slip area. While coseismic slip inversions produced by different teams differ significantly, the spatial complementarity between low and high frequency slip is a common feature well illustrated by this particular slip model. Kinematic source inversions constrained by global teleseismic data, which are dominated by frequencies lower than 0.1 Hz for this earthquake, also place most of the low

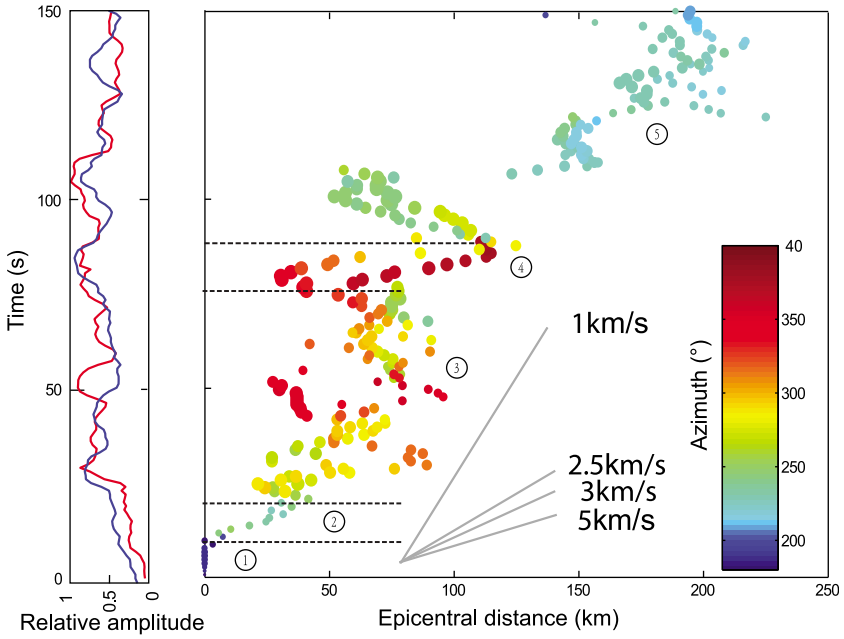

Figure 2. Rupture time versus epicentral distance. The timing of the high frequency radiators seen by both arrays are plotted against their epicentral distance. The color denotes their azimuth with respect to the epicenter and the size of the circles denotes their relative amplitude normalized by the maximum amplitude during the event. The numbers in circles mark the five phases with distinct rupture behavior discussed in section 3. The left panel shows the temporal evolution of normalized amplitudes estimated at the USarray (blue) and at the European network (red). The slope of the gray lines indicate rupture speeds of 1 km/s (slow), 2.5 km/s, 3 km/s (regular) and 5 km/s (super-shear). For reference, the local crust S wave velocity is 3.42 to 4.5 km/s [*Takahashi et al.*, 2004].

frequency (LF) slip updip from the hypocenter (http://www.geol.ucsb.edu/faculty/ji/big_earthquakes/2011/03/0311_v11/honshu_I1.html). This observation is not affected by the uncertainty in the hypocenter location. We found no secondary HF source between the trench and the hypocenter. Moreover, our back-projection analysis at lower frequencies, down to 0.125 Hz (Figure S8 of the auxiliary material), the minimum frequency that allows reasonable temporal resolution, does not show a conclusive trend towards shallower slip. This suggests that slip in the shallower regions of the megathrust interface generated much weaker seismic wave radiation at periods shorter than 10 s.

3. The Spatio-Temporal Evolution of the Tohoku Earthquake

[5] The spatio-temporal evolution of the strongest HF radiations is indicated in Figure 1a. Sustained and energetic HF radiation is reliably imaged by our array back-projections during the first 150 seconds of the rupture. The overall extent of HF rupture size during this period indicates a low average rupture speed. However, rupture speed was highly variable, with several stages of slow, fast and extremely fast rupture. A summary plot of rupture time as a function of epicentral distance, shown in Figure 2 and Figure S8 of the auxiliary material (plotted along dip and strike), provides a more quantitative appreciation of the rupture speed and allows the identification of several distinct stages of the rupture process. Finer details can be observed in the back-projection imaging snapshots (Figure 3) and movies (Animations S1 and S2 of the auxiliary material), including simultaneous but weaker HF sources. The HF rupture initially propagates down-dip

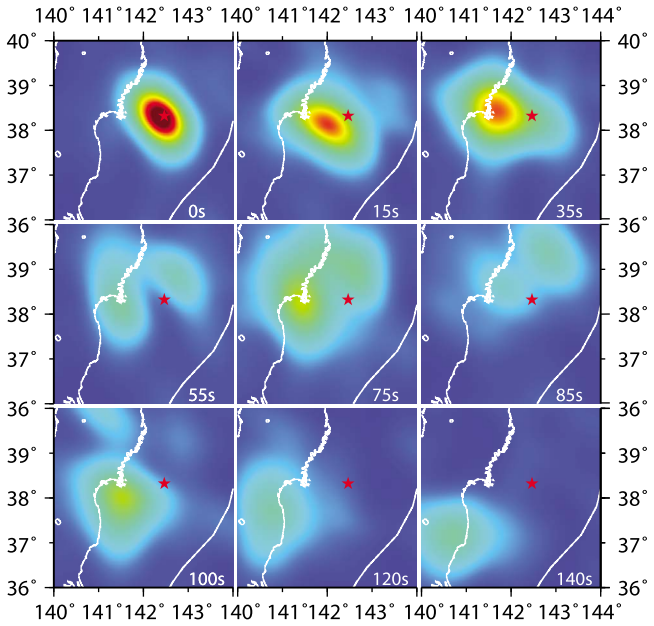

Figure 3. Back projection images every 20 seconds. Colors show the amplitude of the MUSIC pseudo-spectrum. The warmer colors indicate the location of the dominant high frequency radiation sources. The additional snapshot at 90 seconds contains a supershear front to the north. The red star denotes the mainshock epicenter and small white dots the epicenters of aftershocks with magnitude larger than 6 within the first two days. The thick white line represents the trench.

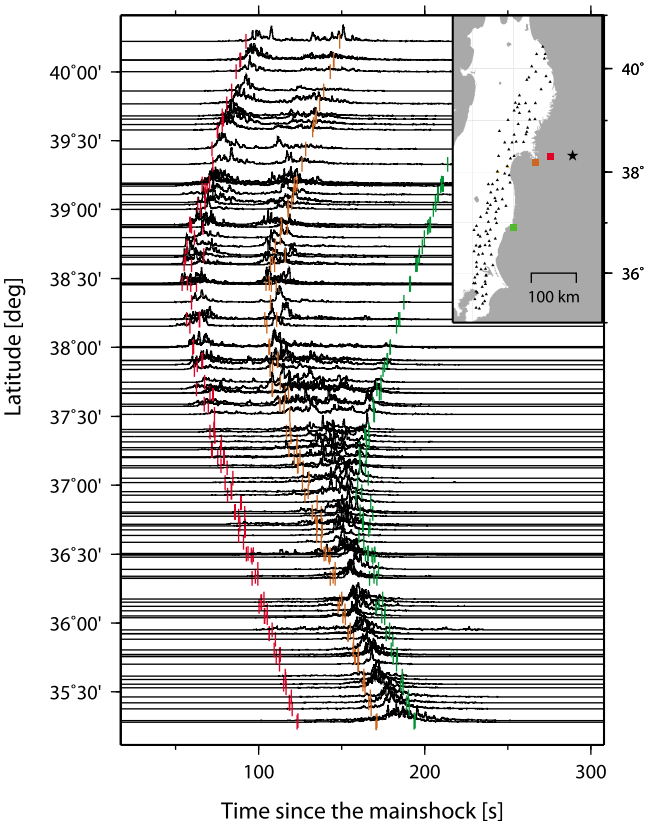

Figure 4. Signatures of the rupture process in the near-source strong motion recordings. Smoothed high-frequency (5–10 Hz) horizontal energy envelopes of strong motion data recorded along the north-eastern coast of Honshu. The selected stations are shown by triangles in the inset map. Traces are scaled by their maximal amplitude. Red, yellow and green vertical bars along the time series indicate the S-wave travel times from high-frequency sources inferred by the back-projection analysis. These ruptured 33 s, 85 s and 140 s after the mainshock origin time, respectively. Their locations are indicated by squares of the respective color in the inset map. The star denotes the mainshock epicenter.

for about 100 seconds, and then splits up into bilateral rupture along strike. The down-dip propagation stage starts with a slow phase: the centroid of HF radiation stalls in a confined area and the source power increases gradually for about 10 seconds (phase 1 indicated in Figure 2). This initiation culminates in a definite change of rupture speed. In the subsequent stage (phase 2) the rupture propagates towards the West at usual speeds of order 3 km/s for about 20 seconds. The rupture then slows down to less than 1 km/s or even ceases for about one minute (phase 3). In Figure 2 the HF source positions show wide azimuthal fluctuations but very slow advance in epicentral distance during this phase. The complex structure of this slow stage is most clearly visualized in the back-projection movies derived from the European array (Animation S2 of the auxiliary material). Figure 3 shows two simultaneous HF sources active at t = 55, 75 and 85 s that delineate an arcuate shaped front. The rupture appears as a rich sequence of bursts generated along the rim of a slowly expanding circular front. The slow front is centered significantly down-dip from the hypocenter, which produces episodes of apparent back-propagation. On the other hand, most low frequency slip occurs in the same stage but mainly located up-dip direction from the hypocenter (http://www.geol.ucsb.edu/faculty/ji/big_earthquakes/2011/03/0311_v11/honshu_I1.html). By the end of the slow stage, at about 80 seconds, an extremely fast rupture detaches towards the North, with apparent supershear speed of order 5 km/s (phase 4), given the local crust S wave velocity is 3.42–4.5 km/s [*Takahashi et al.*, 2004]. Finally a fast rupture front propagates towards the South running at speeds of order 2.5 km/s for more than 100 km (phase 5).

4. Signatures of the Rupture Process in the Strong Motion Data

[6] We inspected the near-source ground motions recorded by dense strong motion networks in Japan to identify the local signature of the features we observed at teleseismic distances. We analyzed recordings of 64 surface and 42 borehole accelerometers located along the north-eastern coast of Honshu. We band-pass filtered the traces in various frequency bands, integrated to velocity and computed smoothed S wave energy envelopes (Figure S9 of the auxiliary material). Figure 4 shows 5–10 Hz envelopes as a function of station latitude. Amplitudes are normalized to emphasize the arrival time moveout of the main strong motion phases. Three episodes are prominent, two in the North, consistent with sources near the hypocentral latitude, and one far South near the end of the rupture. We trace rays from the HF source locations determined by the back-projection analysis to the strong motion stations, using a 1D velocity model derived from local seismic profiles [*Takahashi et al.*, 2004]. The three prominent bursts are thus associated to HF phases observed at teleseismic distances. The colored vertical short bars in Figure 4 indicate the S-wave arrival times from locations that ruptured 33, 85 and 140 seconds after the mainshock origin time. These correspond, respectively, to the end of the first fast rupture stage, the beginning of the extremely fast northwards rupture and the approach to the southern end of the rupture. The strong motions are intermittent in Miyagi and more sustained along Fukushima, reflecting the contrasted character of these two portions of the rupture process (phase 3 and 5, respectively).

5. Discussion

[7] Our results highlight the spatial complementarity between low and high frequency source properties of the Tohoku earthquake, as also discussed elsewhere [*Simons et al.*, 2011]. This phenomenon has been reported for several other earthquakes, although not systematically [*Nakahara*, 2008]. HF is radiated by fast changes in rupture speed or in slip. These changes can be due to the presence of frictional heterogeneities in the brittle-ductile transitional regions at the base of the seismogenic zone, stopping phases radiated from abrupt rupture arrest, strong phases radiated when the rupture front encounters residual stress concentrations left by previous earthquakes [*Madariaga*, 1983] and dynamic triggering of crustal faults above the mega-thrust. A natural generalization of this HF/LF complementarity to

intermediate frequencies poses a cautionary note for source inversion studies that combine geodetic and seismological data, which are sensitive to different frequencies. The relation between HF and LF source radiation also provides an observational constraint on kinematic source models for broadband ground motion prediction and urges for the integration of physics-based rupture models into those methodologies [*Pulido and Dalguer*, 2009].

[8] Our analysis reveals the seismic signature of a slow initiation of the Tohoku-Oki earthquake rupture. We used only the European data to resolve this initiation phase, since the USarray is at a P nodal direction and dominated by the sP phase which complicated the initial waveforms. Back-projection of the initial portions of the waveforms was done with short (5 s long) sliding windows. Extrapolating in Figure 2 the moveout of the HF sources during "phase 2" down to zero distance unambiguously reveals an initial rupture delay longer than the analysis window. Local strong motion recordings are deficient in high frequency content during the first 10 s [*Hoshiba and Kazuhiro*, 2011], independently implying a slow initiation. A progressive transition to dynamic rupture has been observed in laboratory experiments [*Nielsen et al.*, 2010; *Ohnaka and Kuwahara*, 1990; *Okubo and Dieterich*, 1984] and predicted by theoretical models [*Ampuero and Rubin*, 2008; *Dieterich*, 1992; *Lapusta and Rice*, 2003], but has eluded unambiguous seismological observations at natural scales. Whether this initiation stage is subtended by an aseismic nucleation process or results from a cascade of triggering between seismic subevents [*Ellsworth and Beroza*, 1995] cannot be resolved by our analysis. The duration of the observed slow initiation stage (less than 10 s) is consistent with the empirical scaling relation between nucleation phase duration and seismic moment proposed by [*Ellsworth and Beroza*, 1995], although somewhat shorter suggesting a break in scaling at very large magnitudes possibly due to saturation of the seismogenic depth. Further studies of the nucleation of the Tohoku earthquake are warranted, including imaging of its early stages based on empirical Green's functions [*Shibazaki et al.*, 2002; *Uchide and Ide*, 2007] and analysis of its foreshock sequence [*Bouchon et al.*, 2011].

[9] During the second slow rupture stage of the Tohoku earthquake (phase 3 in Figure 2), the macroscopic rupture front almost comes to a halt and then restarts. This stage provides another potential window into the factors controlling earthquake nucleation and arrest, especially under transient stressing conditions. A similar slow rupture stage with apparent speed of order 1 km/s was inferred between two main asperities during the 2007 Pisco earthquake, offshore Peru [*Perfettini et al.*, 2010]. However, the scarcity of data recorded for that event did not allow resolving whether the long delay between the two main subevents was due to a slow rupture or to a delayed triggering process. For the Tohoku earthquake the migration pattern of the HF radiation during the slow stage is consistent with triggering along the rim of a slow rupture front. This slow stage could be related to propagation over a transition region between brittle and ductile fault behavior that separates the hypocentral region from the slip regions of the 1978 and 2005 Miyagi-Oki earthquakes. We picture this as a rheologically heterogeneous region made of a ductile fault matrix interspersed with compact brittle asperities capable of generating HF radiation. This patchy view of the brittle-ductile transition zone is consistent with the observation of clusters of repeating earthquake in Tohoku [*Igarashi et al.*, 2001], and is analogous to a current interpretation of the environment where coupled slow slip and tremor processes occur [*Ito et al.*, 2007]. Moreover, throughout the rest of the rupture the HF sources coincide with the down-dip end of the background interplate seismicity [*Igarashi et al.*, 2001]. In an alternative interpretation, the rupture slowed down as it propagated over regions of low stress within the slip area of the 1978 and 2005 Miyagi earthquakes, but radiated HF as it hit the stress concentrations left at the edges of those same events. Similarly, the final rupture stage towards the South delineates the bottom edge of historical earthquakes off-Fukushima. Yet another possibility is that the dynamic stress transfer from a slow megathrust rupture (deficient in HF) triggered brittle rupture (rich in HF) on faults in the overriding plate. A finer resolution study of the depth and focal mechanism of the HF sources, aftershocks and repeating earthquakes might help discriminating these interpretations.

[10] The stage of extremely fast rupture towards the North is most clearly visible by the European array, which has better resolution in the along-strike direction. This stage could correspond to a supershear rupture front. Its speed is comparable to $\sqrt{2}$ times the S wave speed, a stable speed in dynamic models of supershear rupture [*Rosakis*, 2002]. A subshear front hitting obliquely into a barrier is an alternative interpretation, but that would generate an apparent speed in the observed range only under very restrictive conditions. Alternatively, dynamic triggering would create an apparent supershear phenomena, since the back-projection tends to image apparent secondary sources with small power connecting true sources (Figure S7 of the auxiliary material). This artifact is unlikely for the Tohoku-Oki earthquake, since the power is almost uniform during the supershear stage. However, the very fast front propagates mainly along strike and existing theoretical models do not allow supershear ruptures in mode III. Along-strike supershear rupture in subduction earthquakes requires a significant along-strike slip component or yet unexplored mode coupling processes that efficiently break the mode III symmetries. While the second strong phase observed in the strong motion data can be associated to the HF radiation found in dynamic rupture models during the transition to supershear speeds, this is not a unique interpretation. Further signatures of supershear propagation might be found in the local strong motion data if there is significant Mach cone radiation towards the land. Ocean bottom pressure gauges that recorded HF acoustic signals, especially stations TM1 and TM2, could also provide precious insight into this question.

[11] Our observations provide an overview of the complicated rupture process of the Tohoku-Oki earthquake and virtually constitute, in a single event, a catalog of the broad spectra of earthquake phenomenology. We highlighted here key features of relevance for earthquake dynamics. These are potential targets for further efforts to assimilate the wealth of data related to this mega-earthquake, with the ultimate goal of understanding the relations between earthquake complexity and the heterogeneous and multi-scale structure of active fault zones.

[12] **Acknowledgments.** This research was supported by NSF grant EAR-1015704, by the Gordon and Betty Moore Foundation, and by the

Southern California Earthquake Center, which is funded by NSF cooperative agreement EAR-0106924 and USGS cooperative agreement 02HQAG0008. This paper is Caltech Tectonics Observatory contribution #173 and Caltech Seismolab contribution SCEC #1501.

[13] The Editor thanks Jon Fletcher and an anonymous reviewer for their assistance in evaluating this paper.

References

Ampuero, J. P., and A. M. Rubin (2008), Earthquake nucleation on rate and state faults aging and slip laws, *J. Geophys. Res.*, *113*, B01302, doi:10.1029/2007JB005082.

Bernard, P., and R. Madariaga (1984), A new asymptotic method for the modeling of near-field accelerograms, *Bull. Seismol. Soc. Am.*, *74*(2), 539–557.

Borcea, L., G. Papanicolaou, and C. Tsogka (2005), Interferometric array imaging in clutter, *Inverse Probl.*, *21*(4), 1419–1460, doi:10.1088/0266-5611/21/4/015.

Bouchon, M., H. Karabulut, M. Aktar, S. Ozalaybey, J. Schmittbuhl, and M. P. Bouin (2011), Extended nucleation of the 1999 M-w 7.6 Izmit earthquake, *Science*, *331*(6019), 877–880, doi:10.1126/science.1197341.

Dieterich, J. H. (1992), Earthquake nucleation on faults with rate-dependent and state-dependent strength, *Tectonophysics*, *211*(1–4), 115–134, doi:10.1016/0040-1951(92)90055-B.

Ellsworth, W. L., and G. C. Beroza (1995), Seismic evidence for an earthquake nucleation phase, *Science*, *268*(5212), 851–855, doi:10.1126/science.268.5212.851.

Fletcher, J. B., P. Spudich, and L. M. Baker (2006), Rupture propagation of the 2004 Parkfield, California, earthquake from observations at the UPSAR, *Bull. Seismol. Soc. Am.*, *96*(4B), S129–S142, doi:10.1785/0120050812.

Goldstein, P., and R. J. Archuleta (1991), Deterministic frequency-wavenumber methods and direct measurements of rupture propagation during earthquakes using a dense array: Theory and methods, *J. Geophys. Res.*, *96*(B4), 6173–6185, doi:10.1029/90JB02123.

Hoshiba, M., and I. Kazuhiro (2011), Initial 30 seconds of the 2011 off the Pacific coast Tohoku earthquake (Mw 9.0)-amplitude and τc for magnitude estimation for earthquake early warning, *Earth Planets Space*, doi:10.5047/eps.2011.06.015, in press.

Igarashi, T., T. Matsuzawa, N. Umino, and A. Hasegawa (2001), Spatial distribution of focal mechanisms for interplate and intraplate earthquakes associated with the subducting Pacific plate beneath the northeastern Japan arc: A triple-planed deep seismic zone, *J. Geophys. Res.*, *106*(B2), 2177–2191, doi:10.1029/2000JB900386.

Ishii, M., P. M. Shearer, H. Houston, and J. E. Vidale (2005), Extent, duration and speed of the 2004 Sumatra-Andaman earthquake imaged by the Hi-Net array, *Nature*, *435*(7044), 933–936.

Ito, Y., K. Obara, K. Shiomi, S. Sekine, and H. Hirose (2007), Slow earthquakes coincident with episodic tremors and slow slip events, *Science*, *315*(5811), 503–506, doi:10.1126/science.1134454.

Lapusta, N., and J. R. Rice (2003), Nucleation and early seismic propagation of small and large events in a crustal earthquake model, *J. Geophys. Res.*, *108*(B4), 2205, doi:10.1029/2001JB000793.

Madariaga, R. (1983), High-frequency radiation from dynamic earthquake fault models, *Ann. Geophys.*, *1*(1), 17–23.

Nakahara, H. (2008), Seismogram envelope inversion for high-frequency seismic energy radiation from moderate-to-large earthquakes, *Adv. Geophys.*, *50*, 401–426, doi:10.1016/S0065-2687(08)00015-0.

Nielsen, S., J. Taddeucci, and S. Vinciguerra (2010), Experimental observation of stick-slip instability fronts, *Geophys. J. Int.*, *180*(2), 697–702, doi:10.1111/j.1365-246X.2009.04444.x.

Ohnaka, M., and Y. Kuwahara (1990), Characteristic features of local breakdown near a crack-tip in the transition zone from nucleation to unstable rupture during stick-slip shear failure, *Tectonophysics*, *175*(1–3), 197–220, doi:10.1016/0040-1951(90)90138-X.

Okubo, P. G., and J. H. Dieterich (1984), Effects of physical fault properties on frictional instabilities produced on simulated faults, *J. Geophys. Res.*, *89*(B7), 5817–5827.

Perfettini, H., et al. (2010), Seismic and aseismic slip on the central Peru megathrust, *Nature*, *465*(7294), 78–81, doi:10.1038/nature09062.

Pulido, N., and L. A. Dalguer (2009), Estimation of the high-frequency radiation of the 2000 Tottori (Japan) earthquake based on a dynamic model of fault rupture: Application to the strong ground motion simulation, *Bull. Seismol. Soc. Am.*, *99*(4), 2305–2322, doi:10.1785/0120080165.

Rosakis, A. J. (2002), Intersonic shear cracks and fault ruptures, *Adv. Phys.*, *51*(4), 1189–1257, doi:10.1080/00018730210122328.

Rost, S., and C. Thomas (2002), Array seismology: Methods and applications, *Rev. Geophys.*, *40*(3), 1008, doi:10.1029/2000RG000100.

Schmidt, R. O. (1986), Multiple Emitter Location and Signal Parameter-Estimation, *IEEE Trans. Antennas Propag.*, *34*(3), 276–280, doi:10.1109/TAP.1986.1143830.

Shibazaki, B., Y. Yoshida, M. Nakamura, M. Nakamura, and H. Katao (2002), Rupture nucleations in the 1995 Hyogo-ken Nanbu earthquake and its large aftershocks, *Geophys. J. Int.*, *149*(3), 572–588, doi:10.1046/j.1365-246X.2002.01601.x.

Simons, M., et al. (2011), The 2011 magnitude 9.0 Tohoku-Oki Earthquake: Mosaicking the megathrust from seconds to centuries, *Science*, *332*, 1421–1425, doi:10.1126 science.1206731.

Spudich, P., and L. N. Frazer (1984), Use of ray theory to calculate high-frequency radiation from earthquake sources having spatially-variable rupture velocity and stress drop, *Bull. Seismol. Soc. Am.*, *74*(6), 2061–2082.

Takahashi, N., S. Kodaira, T. Tsuru, J. O. Park, Y. Kaneda, K. Suyehiro, H. Kinoshita, S. Abe, M. Nishino, and R. Hino (2004), Seismic structure and seismogenesis off Sanriku region, northeastern Japan, *Geophys. J. Int.*, *159*(1), 129–145, doi:10.1111/j.1365-246X.2004.02350.x.

Uchide, T., and S. Ide (2007), Development of multiscale slip inversion method and its application to the 2004 mid-Niigata Prefecture earthquake, *J. Geophys. Res.*, *112*, B06313, doi:10.1029/2006JB004528.

J.-P. Ampuero, A. Inbal, and L. Meng, Seismological Laboratory, California Institute of Technology, 1200 E. California Blvd., MS 252-21 South Mudd Bldg., Rm. 364, Pasadena, CA 91125, USA. (lsmeng@gps.caltech.edu)